An efficient multi-stage algorithm for full calibration of the hemodynamic model from BOLD signal responses

Brian Zambri[1], Rabia Djellouli[1*], and Taous-Meriem Laleg-Kirati[2]

[1]*Department of Mathematics & Interdisciplinary Research Institute for the Sciences, California State University, Northridge, 18111 Nordhoff St, Northridge, CA, 91330, USA*

[2]*Computer, Electrical and Mathematical Science and Engineering (CEMSE) Division, King Abdullah University of Science and Technology, Thuwal 23955-6900, KSA*

SUMMARY

We propose a computational strategy that falls into the category of prediction/correction iterative-type approaches, for calibrating the hemodynamic model introduced by Friston et al. (2000). The proposed method is employed to estimate consecutively the values of the biophysiological system parameters and the external stimulus characteristics of the model. Numerical results corresponding to both synthetic and real functional Magnetic Resonance Imaging (fMRI) measurements for a single stimulus as well as for multiple stimuli are reported to highlight the capability of this computational methodology to fully calibrate the considered hemodynamic model.

Received . . .

KEY WORDS: hemodynamic model; parameter estimation; inverse problem

1. INTRODUCTION

In spite of its essential role, the brain remains by far the most enigmatic organ of the human body. In an effort to better understand the development and function of this vital organ, vast, worldwide

*Correspondence to: Department of Mathematics, California State University, Northridge, 18111 Nordhoff St. Northridge, CA, 91324, USA. E-mail: rabia.djellouli@csun.edu

This article has been accepted for publication and undergone full peer review but has not been through the copyediting, typesetting, pagination and proofreading process, which may lead to differences between this version and the Version of Record. Please cite this article as Int. J. Numer. Meth. Biomed. Engng., e02875. doi: 10.1002/cnm.2875

research programs have been launched in the past two decades, led by the latest major initiatives: the Human Brain Project (HBP) by the European Union [1] and Brain Research through Advancing Innovative Nanotechnologies (BRAIN) by the United States [2].

Mathematical modeling of event-related brain activity can be an attractive alternative tool for monitoring and possibly predicting brain activity, with the potential to provide early diagnosis and treatment of brain disorders. The determination of such a comprehensive mathematical model remains, however, an outstanding problem. Indeed, much debate has arisen from issues including the nonlinearity of brain activity, a coupling or uncoupling of cerebral blood flow and oxygen metabolism [3], and the inclusion of metabolic effects [4]. As a result, two distinct approaches have emerged–General Linear Modeling (GLM) and Nonlinear physiological Modeling (NLM)–in attempt to describe the hemodynamic response during brain activation. GLM involves statistical analysis, whereby a predefined kernel is used to assess the convolution of the neural activity. The kernel–known as the Hemodynamic Response Function (HRF)–has been defined using several different basis functions, including Poisson [5], Gaussian [6], Gamma [7, 8], and inverse Logit [9] functions. The problem with the linear approach is that it is blind to the physiological causes of the transient aspects of the functional Magnetic Resonance Imaging (fMRI) output, the Blood Oxygenation-Level Dependent (BOLD) signal. In addition, nonlinear activity in the BOLD signal has been observed on multiple occasions [3,10–12]. These severe limitations in GLM gave rise to the nonlinear approach to modeling neural activity [3,13], in which the venous compartment is modeled as a balloon that expands to account for the increased blood flow that occurs during local activation. The increase in blood flow results in a local decrease in deoxyhemoglobin concentration, and a corresponding increase in the BOLD signal [13]. This new characterization of the BOLD signal's dependence on cerebral blood flow, volume, and deoxyhemoglobin content was made complete with the introduction of the flow-inducing signal [14], which serves as the link between neuronal activation and the associated changes in local cerebral blood dynamics.

The hemodynamical model that we consider here was first introduced in [3]. The model is a dynamical system which includes a first-order nonlinear differential system, known as the Balloon model [3, 14]. This differential system is coupled with a nonlinear equation which represents the BOLD Signal [3]. The brain response characterized by this model is sensitive to the biophysiological parameters of the system as well as to its control functions representing the external stimuli during brain activation. In practice, the values of these parameters are not accessible via lab measurements. Hence, accurately estimating these values is a prerequisite step for successfully monitoring brain activity by using the considered hemodynamical model. This step, called the model calibration, is not a trivial task. Indeed, it consists of solving an inverse problem which falls into the category of parameter estimation of differential operators. This inverse problem is difficult to solve both

mathematically and numerically, due to its nonlinear and ill-posed aspects. Extensive efforts have been made to address these difficulties, though with only limited success. Indeed, most existing numerical methods (see, e.g., [14–21]) either use high precision on the parameters prior variance or assume known neural input. Additionally, most of these methods require prior knowledge about the shape, duration, and amplitude of the neural activity in the brain, which is not easy to infer for complex event-related fMRI experiments. In [17], a local linearization filter (LLF) was used to estimate the hidden states and parameters of the hemodynamic model. It also estimates the hidden neural activity using a fixed number of radial basis functions. However, a priori information about the neural input was used to constrain the ill-posed inverse problem. In [22], dynamic expectation maximization (DEM) method, a variational Bayesian technique, was used to estimate hidden model parameters and states. In an empirical setting, it has been also used to de-convolve neuronal activity from observed hemodynamic responses in the brain. DEM was shown to be more robust than the extended Kalman and particle filters. However, it was shown that Cubature Kalman filter (CKF) and its square root form out-performs the DEM. The work in [23] describes a nonlinear neural network procedure for hemodynamic de-convolution under known parameters. It estimates both input and states, but not the parameters. Hence, these methods were designed for *partial* model calibration and not for solving the real-world problem: the *full* inverse problem. Last, but not least, most of these methods (see, e.g., [14–20]) are even unable to accurately estimate the biophysiological parameters without a priori knowledge on the values of the sought-after parameters. This constitutes a major drawback, since these parameters cannot, in practice, be measured within any interval of confidence. The Tikhonov-regularized Newton Method with Cubature Kalman Filtering (TNM-CKF), the latest iterative method developed in [21], is able to successfully retrieve the biophysiological parameters without any a priori knowledge on their values. In spite of its impressive accuracy performance, TNM-CKF fails dramatically, as demonstrated in Section 3, to achieve full model calibration, that is, to estimate simultaneously the two sets of parameters: the biophysiological parameters and the control function parameters.

Given these considerations, we propose a new computational strategy for estimating the two sets of parameters that characterize the hemodynamic model [3, 14]. Since the two sought-after sets of parameters are of a different nature and, in general, even of a different scale, our idea is to adopt a prediction/correction-type approach to estimate these two sets of parameters. More specifically, we propose a multi-step strategy that employs–at each step–the TNM-CKF algorithm to estimate (predict and correct) the values of one set of parameters while the values of the other set remain "frozen." The importance of this new procedure is two-fold: First, the method calibrates the hemodynamic model without any a priori knowledge of the values of the biophysiological parameters *and* characterizes the underlying neuronal activity without knowledge of the input, as

demonstrated in Section 4.1. Second, the method's ability to characterize a single event can be extended to distinguish and characterize *multiple* distinct events in a single subject, as demonstrated in Section 4.2.

The remainder of this paper is organized as follows: in Section 2, we first introduce the mathematical model that describes changes in the brain in response to an exogeneous stimulus during brain activation. This model describes a forward problem. Then, we formulate the inverse problem which consists of determining the biophysiological parameters of the system as well as the characteristics of the considered stimuli. Section 3 is dedicated to the presentation of the proposed solution methodology and to highlighting its main features. In Section 4, we assess the performance of the proposed solution methodology. To this end, we present numerical results corresponding to both synthetic and real data. Finally, we present a summary and closing remarks in the Conclusion.

2. THE MATHEMATICAL MODEL: DIRECT AND INVERSE FORMULATION

2.1. *Nomenclature and Assumptions*

Throughout this paper, we adopt the following notations and hypotheses:

- t is a nonnegative real number which represents time.
- Δt is a positive real number representing the chosen time step.
- $t_n = n\Delta t$ represents the time at step n.
- $\vec{x}(t) = (x_1(t), x_2(t), x_3(t), x_4(t))^T \in \mathbb{R}^4$ is the state vector function whose coordinates are [14]:
  - $x_1(t)$, the normalized cerebral blood flow (CBF)
  - $x_2(t)$, the flow inducing signal
  - $x_3(t)$, the normalized cerebral blood volume (CBV)
  - $x_4(t)$, the normalized total deoxyhemoglobin content level
- $\vec{x}_0$ is the initial state vector. $\vec{x}_0 = \vec{x}(0) = (1, 0, 1, 1)^T$, which indicates that the brain is initially fully at rest.
- $y(t)$ is a real-valued function representing the measured BOLD signal
- $\vec{\theta} = (\theta_1, \theta_2, \theta_3, \theta_4, \theta_5, \theta_6, \theta_7)^T \in \mathbb{R}^7$ is the biophysiological parameters vector whose coordinates are [14]:
  - θ_1, the reciprocal of the stiffness exponent
  - θ_2, the neural efficacy
  - θ_3, the rate of signal decay

  - θ_4, the rate of flow-dependent elimination
  - θ_5, the reciprocal of the hemodynamic transit time
  - θ_6, the resting net oxygen extraction
  - θ_7, the resting blood volume

- ν_t represents the noise at time t in the process equation. ν_t is a random Gaussian vector with zero mean and covariance Q_t, a 4x4 positive semidefinite matrix.
- ω_t represents the noise at time t in the measurement equation. ω_t is a random Gaussian vector with zero mean and covariance R_t, a real-valued scalar.
- $u(t, \vec{p})$ is the external stimulus–or control function–at time t. Here, we consider an *On-Off* stimulus, that is, u is given by:

$$u(t) = a \cdot \chi \left(\frac{t - \widehat{T}_{\text{on}}}{T_{\text{off}} - T_{\text{on}}} \right), \tag{1}$$

where a represents the intensity of the stimulus and χ is the indicator function for the interval $[0, 1]$. $\widehat{T}_{\text{on}} = T_{\text{on}} + \delta_t$ (resp. $\widehat{T}_{\text{off}} = T_{\text{off}} + \delta_t$), where T_{on} (resp. T_{off}) represents the start (resp. end) time of the stimulus, and δ_t is the delay time between the neuronal activity and the CBF response. This delay is introduced as δt_f in [24], and is implemented with a convolution of the neural activity in the expression of the cerebral blood flow (see Equation (13) in [24]). Here, we suggest to implement the delay as part of the stimulus function. Note that, in general, δ_t is considered to be a biophysiological parameter since it depends on the subject and not on the stimulus. We denote by $\vec{p} = (a, \widehat{T}_{\text{on}}, \widehat{T}_{\text{off}})^T$ the vector of parameters characterizing the considered external stimulus, also called the control input. Note that the vector $\vec{p}$, along with biophysiological parameter vector $\vec{\theta}$, are the parameters to be fit.

2.2. *The Direct Problem: The Hemodynamic Model*

The mathematical model that describes the hemodynamic activity of the brain in response to a single exogenous input known as the hemodynamic model (HDM) was first developed by Buxton et al. [3]. Friston et al. [14] further advanced the model by elucidating the relationship between the neuronal activity and the induced CBF changes. The entire pathway from the neural activity to the BOLD signal is described by a first-order, nonlinear differential system coupled with a nonlinear algebraic equation. The HDM is given by:

$$\text{(HDM)} \begin{cases} \dot{\vec{x}}(t) = A(\vec{x}(t), u(t, \vec{p}), \vec{\theta}) + \nu_t \\ y(t) = B(\vec{x}(t), \vec{\theta}) + \omega_t \qquad ; t \geq 0 \\ \vec{x}(0) = \vec{x}_0 \end{cases} \tag{2}$$

where the vector-valued function A is given by:

$$A(\vec{x}(t), u(t,\vec{p}), \vec{\theta}) = \begin{cases} x_2(t) \\ \theta_2 u(t,\vec{p}) - \theta_3 x_2(t) - \theta_4(x_1(t)-1) \\ \theta_5\left(x_1(t) - x_3^{\theta_1}(t)\right) \\ \theta_5\left(x_1(t)\frac{1-(1-\theta_6)^{1/x_1(t)}}{\theta_6} - x_3^{(\theta_1-1)}(t)x_4(t)\right) \end{cases}, \tag{3}$$

and the real-valued function B represents the BOLD signal. The function B is given by:

$$B(\vec{x}(t), \vec{\theta}) = \theta_7\left[7\theta_6(1-x_4(t)) + 2\left(1 - \frac{x_4(t)}{x_3(t)}\right) + (2\theta_6 - 0.2)(1-x_3(t))\right]. \tag{4}$$

The following remarks are of importance to the system:

- The differential system of HDM describes the underlying physics of the continuous hemodynamic system, i.e., the Balloon model.
- The algebraic equation of HDM models the observations, that is, the BOLD signal, as a volume-weighted sum of the extravascular and intravascular signal.
- The third equation of HDM is the initial state vector, which describes the initial state of brain activity.

Furthermore, the ordinary differential system of HDM is composed of four coupled differential equations as indicated by (3), which model the following:

- The first equation represents the rate of change of normalized cerebral blood flow.
- The second equation describes the rate of change of the flow-inducing signal, and is assumed to include within it neurogenic and diffusive signal subcomponents [14].
- The third equation models the rate of change of normalized cerebral blood volume.
- The fourth equation characterizes the rate of change of normalized total deoxyhemoglobin content.

2.3. The Inverse Problem: Parameter Estimation

As stated in the Introduction, our aim is to propose an efficient solution methodology for computing the biophysiological parameter vector $\vec{\theta}$ together with all the external stimuli characteristics $\vec{p}_j$; $j = 1, \ldots, M$, where M designates the number of considered events, from the knowledge of some BOLD signal measurements. We must emphasize that all existing numerical procedures have been designed to evaluate one set of parameters only (either $\vec{\theta}$ or $\vec{p}_j$) while assuming the others to be known. To the best of our knowledge, this is the first time where the problem of fully calibrating HDM 2 is considered. To formulate mathematically this inverse problem, we first observe that

the direct problem HDM 2 defines a nonlinear operator, $\mathcal{F}$, which maps $(\vec{\theta}, \vec{p}_j)$ to the BOLD signals y_j. Therefore, the problem of simultaneously determining the biophysiological parameters $\vec{\theta}$ and the external stimulus characteristics $\vec{p}_j$ from the knowledge of measured BOLD signals $\widetilde{y}_j$– corresponding to multiple events–can be formulated as the following inverse problem:

$$\begin{cases} \textit{Given an initial measured state } \widetilde{\vec{x}}_0 \textit{ and measured BOLD signals } \widetilde{y}_j \textit{ corresponding} \\ \textit{to } M \textit{ events, find the biophysiological parameters } \vec{\theta}\textit{, the control input parameters } \vec{p}_j, \\ \textit{and the state vector function } \vec{x}_j(t) \textit{ such that:} \\ \qquad \mathcal{F}(\vec{\theta}, \vec{p}_j; \vec{x}_j(t)) = \widetilde{y}_j(t); \qquad j = 1, \ldots, M \end{cases}, \tag{5}$$

where the tilde denotes a noisy quantity. In the case of the initial state, the noise represents some level of activity in the brain, i.e., the brain is not fully at rest. In the case of the BOLD signal, the noise corresponds to possible errors associated with the measurements. Note that the problem defined by Equation 5 is a nonlinear inverse problem, which falls into the category of identifying the parameters of an ordinary differential system. Since in practice the BOLD signal is not known for all time, but rather measured at discrete time points, each BOLD signal is represented here by a vector $\vec{y}_j$ whose coordinates are the measurements at a given (equispaced) time t_k. Therefore, if each BOLD signal is measured at N_m time points, Equation 5 can be re-formulated as:

$$\begin{cases} \textit{Given } \widetilde{\vec{x}}_0 \text{ and } \widetilde{\vec{y}}_j = (\widetilde{y}_{j,0}, \widetilde{y}_{j,1}, \ldots, \widetilde{y}_{j,N_m})^T, \\ \textit{find } \vec{\theta}, \vec{p}_j\textit{, and } \vec{x}_j(t) \textit{ such that:} \\ \mathcal{F}(\vec{\theta}, \vec{p}_j; \vec{x}_j(t_k)) = \widetilde{y}_{j,k}; \quad k = 0, 1, \ldots, N_m,\ j = 1, \ldots M \end{cases} \tag{6}$$

Consequently, solving the inverse problem 6 leads to the calibration of HDM 2.

3. SOLUTION METHODOLOGY

We introduce here a new procedure for solving 6 and thus calibrating HDM 2. The method employs the TNM-CKF algorithm in a multi-step framework to successively "predict" and "correct" each set of parameters separately, as described in what follows.

3.1. The Proposed Solution Methodology: A Multi-Step Strategy

As stated earlier in the introduction section, the standard TNM-CKF algorithm presented in [21] is ineffective for estimating the biophysiological parameters when the stimulus characteristics and

the corresponding neuronal activity are assumed to be unknown. Indeed, the results reported in Section 4.1.1 demonstrate that the algorithm fails dramatically to estimate both the biophysiological parameters, $\vec{\theta}$, and the control function parameters, $\vec{p}_j$, simultaneously. This does not seem surprising, since the biophysiological parameter vector $\vec{\theta}$ and the control input characteristics $\vec{p}_j$ are not of the same nature or scale. Their determination in "one shot" appears to be a challenging, if not impossible, task. For this reason, we propose an alternative approach for solving the full inverse problem 6 that is accurate, cost effective, and robust to the noise. The proposed solution methodology is a multi-step strategy that also employs the TNM-CKF procedure, but with a prediction/correction-type approach. More specifically, the proposed iterative procedure–rather than searching for all the parameters simultaneously–consists of "freezing" the value of one parameter vector (either $\vec{\theta}$ or $\vec{p}$), and updating the values of the "free" parameter vector. The proposed algorithm can be summarized as follows (see Fig. 1):

- **Step 0: Intialization.** We start with M sets of BOLD signal measurements, that is $\widetilde{\vec{y}}_j$, $j = 1, \ldots, M$, where M is the number of stimuli, and $\widetilde{\vec{y}}_j$ is the jth BOLD signal measured uniformly at N_m time steps, i.e., $\widetilde{\vec{y}}_j \in \mathbb{R}^{\mathrm{N_m}}$. We fix an initial guess $(\vec{\theta}^{(0)}, \vec{p}^{(0)})$, whose coordinate values are selected arbitrarily in the absence of a priori knowledge on the parameter values. This step can be viewed as a *prediction* of the biophysiological parameters $\vec{\theta}$ and the control function characteristics $\vec{p}$. We must emphasize the fact that the convergence of the proposed solution methodology does not require a priori knowledge on the target parameters, $(\vec{\theta}, \vec{p})$.
- **Step 1: Update the Biophysiological Parameters.** For each measured BOLD signal $\widetilde{\vec{y}}_j$, apply the TNM-CKF algorithm to update $\vec{\theta}_j^{(0)}$. At convergence or stagnation, the TNM-CKF algorithm delivers an updated value, $\vec{\theta}_j^{(m_1)}$.
- **Step 2: Update the Model.** Replace the initial guess $\vec{\theta}_j^{(0)}$ by the computed value $\vec{\theta}_j^{(m_1)}$, that is:

$$(\vec{\theta}_j^{(0)}, \vec{p}_j^{(0)}) \leftarrow (\vec{\theta}_j^{(m_1)}, \vec{p}_j^{(0)}). \tag{7}$$

- **Step 3: Update the Control Function Parameters.** For each measured BOLD signal $\widetilde{\vec{y}}_j$, apply the TNM-CKF algorithm to update $\vec{p}_j^{(0)}$. $\vec{p}_j^{(m_1')}$, the updated values of the control function characteristics is delivered by TNM-CKF at convergence or stagnation.
- **Step 4: Update the Model.** Replace the initial guess $\vec{p}_j^{(0)}$ by the computed value $\vec{p}_j^{(m_1')}$, that is:

$$(\vec{\theta}_j^{(0)}, \vec{p}_j^{(0)}) \leftarrow (\vec{\theta}_j^{(0)}, \vec{p}_j^{(m_1')}). \tag{8}$$

- **Step 5: Convergence Test.** If the relative residual, in the Euclidean norm, on the BOLD signal is higher than a prescribed tolerance (the noise level), go to Step 1. If not, then the following

alternative holds: either $M = 1$ and thus the iterative procedure is terminated, or $M > 1$ and then proceed to Step 6.

- **Step 6: Average the Biophysiological Parameters.** Calculate the average of the M computed vectors:

$$\vec{\theta}_{\text{avg}} = \frac{1}{M}\sum_{j=1}^{M}\vec{\theta}_j. \tag{9}$$

$\vec{\theta}_{\text{avg}}$ is then the sought-after biophysiological parameters vector. Note that since the patient is subject to multiple stimuli characterized by $\vec{p}_j$ $(j = 1, \ldots, M)$, the computed biophysiological parameters vector $\vec{\theta}_j$ for the jth stimulus is therefore an approximation of the sought-after biophysiological parameters vector $\vec{\theta}$. For this reason, we consider the average, $\vec{\theta}_{\text{avg}}$, to be the final approximate value of $\vec{\theta}$.

- **Step 7: Update the Initial Guess.** Replace the current initial guess by the computed values, that is:

$$(\vec{\theta}^{(0)}, \vec{p}_j^{(0)}) \leftarrow (\vec{\theta}_{\text{avg}}, \vec{p}_j^{(0)}). \tag{10}$$

- **Step 8: Update the Control Function Parameters.** Apply TNM-CKF to *correct* $\vec{p}_j^{(0)}$ and obtain $\vec{p}_j^{(\text{comp})}, j = 1, \ldots, M$, the updated values of the control function characteristics delivered by TNM-CKF at stagnation. Update the values of δ_t, the delay time between stimulus onset and CBF response, through the vectors $\vec{p}_j$, and then evaluate the averaged value:

$$\delta_{t,\text{avg}} = \frac{1}{M}\sum_{j=1}^{M}\delta_{t,j}^{(\text{comp})}. \tag{11}$$

3.2. Computational Complexity

The numerical implementation of the proposed solution methodology is to some extent straightforward, in the sense that it is similar to the implementation of the standard TNM-CKF [21]. The only issue that deserves special attention is the computation of the Jacobian entries given by 17 when updating the control function parameters, that is, when $\vec{z} = \vec{p}$. Indeed, this computation requires the derivative of the control input function u, given by 1, which gives rise to the Dirac function δ, as illustrated in Fig. 2. More specifically, we have:

$$\frac{\partial u}{\partial \bar{t}} = -\frac{a}{\kappa}\left(\delta(t-\bar{t}) - \delta(t-(\bar{t}+\kappa))\right) \tag{12}$$

and

$$\frac{\partial u}{\partial \kappa} = -a\frac{t-\bar{t}}{\kappa^2}\left(\delta(t-\bar{t}) - \delta(t-(\bar{t}+\kappa))\right), \tag{13}$$

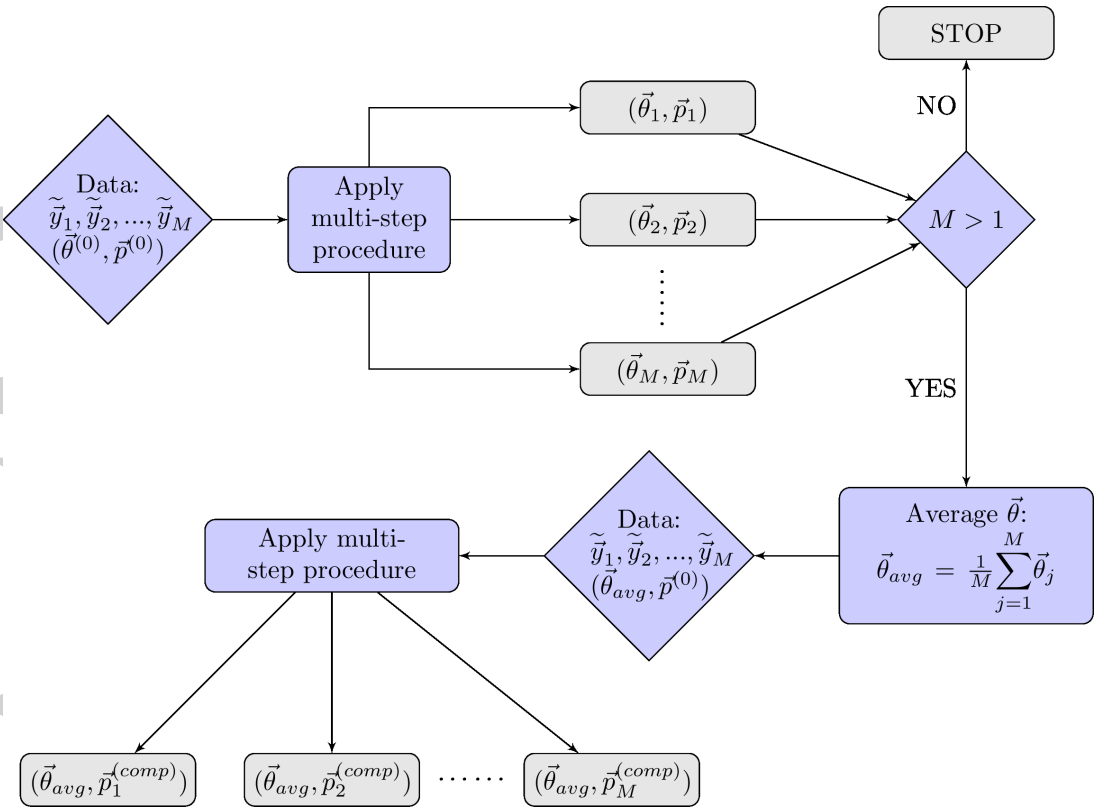

Figure 1. Schematic Diagram for the multi-step algorithm.

where $\bar{t} = \widehat{T}_{\text{on}}$, and $\kappa = T_{\text{off}} - T_{\text{on}}$. The numerical computation of the Dirac delta function when evaluating the Jacobian entries is performed in the context of the finite difference discretization in two stages [25]. First, we approximate the Dirac at a given time t^* by the following Gaussian function:

$$\delta(t - t^*) \approx \frac{1}{\Delta t\sqrt{2\pi}} \exp\left(-\frac{(t - t^*)^2}{2\Delta t^2}\right) \tag{14}$$

This approximation posesses the following two desirable features:

- The integral $\int_{-\infty}^{\infty} \delta(t)dt = 1$ for any choice of Δt.
- $\lim_{\Delta t \to 0} \frac{1}{\Delta t\sqrt{2\pi}} \exp\left(-\frac{t^2}{2\Delta t^2}\right) = \delta(t)$

Then, we use the values of the Gaussian function 14 at time t_i, as illustrated in Fig. 3. Note that there is no need to repeatedly calculate these values. Instead, we form once, at the pre-processing level, a table containing the 21 values in Fig. 3:

$$\vec{\delta} = [\delta_{-10}, \delta_{-9}, \ldots, \delta_9, \delta_{10}]$$

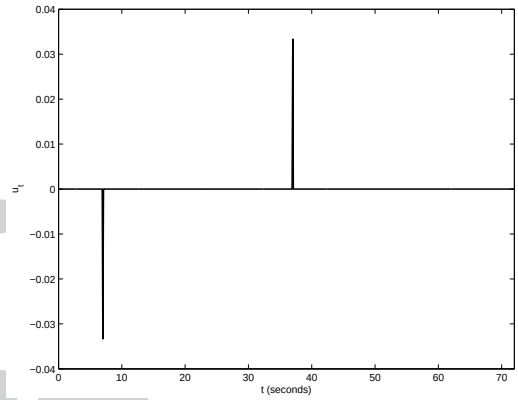

Figure 2. Illustrative representation of the derivative of the control input function u with respect to $\bar{t}$ given by 12, with $\bar{t} = 7$ and $\kappa = 30$.

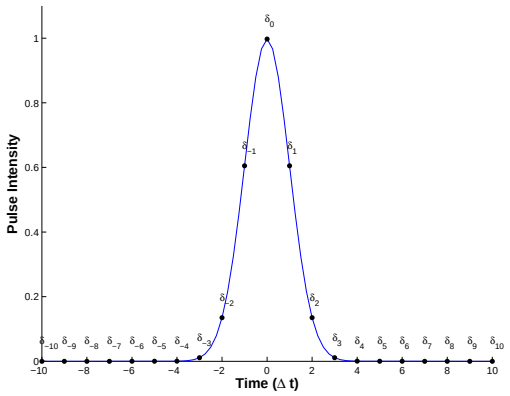

Figure 3. Numerical approximation of the Dirac delta function by the Gaussian function 14 at $t^* = 0$, $\Delta t = 0.4s$, and 21 values measured.

Consequently, the proposed multi-step iterative strategy, outlined in Section 3.1, to estimate the parameters of the HDM 2 given BOLD signal responses corresponding to M events, each with N_m measurements, requires at each iteration m, the following calculations:

- The cubature Kalman filter calls for the solution of one ordinary differential system M times, using $8N_m$ initial values each time, and performing $2N_m M$ Cholesky factorizations of a 4×4 matrix.
- The Regularized Newton algorithm requires solving seven (resp. two) different ordinary differential equations to evaluate the Jacobian matrix of the system to update $\vec{\theta}_j$ (resp. $\vec{p}_j$).
- The determination of the updated values $\delta\vec{\theta}_j^{(m)}$ requires one LU factorization to solve the 7×7 system.
- The computation of the updated values $\delta\vec{p}_j^{(m)}$ requires inverting a 2×2 matrix.
- The computation of $\vec{\theta}_{\text{avg}}$ requires averaging M values of the vector parameter $\vec{\theta}_j$.

4. ILLUSTRATIVE NUMERICAL RESULTS

We present in this section numerical results to illustrate the performance efficiency of the proposed solution methodology for solving the inverse problem 6, and thus for *fully* calibrating HDM 2. These results have been obtained by performing a numerical investigation in which both synthetic and real fMRI data were used. Note that the employed data correspond to either a single stimulus or multiple stimuli. It is important to observe that, in all of the considered numerical experiments, the synthetic BOLD signal measurements have been generated by solving the forward problem given by Equation 2 using the Runge-Kutta method of order 4 [26], whereas a different forward solver–the Fehlberg method [26]–was used in the inversion scheme, in order to avoid the "inverse crime" [27]. The

real measurements correspond to two different experiments: a finger-tapping experiment with one stimulus [23] and a face recognition experiment with four different stimuli [28].

4.1. Experiment 1: Synthetic data corresponding to a single brain activation stimulus

We have performed a numerical investigation using synthetic BOLD signal measurements corresponding to the brain's reaction to a single stimulus. The goal of this study is to analyze the effect on the performance of the algorithm of (a) the noise level in the data and (b) the number of BOLD signal measurements. The results of this study are presented herein.

4.1.1. Robustness of the proposed algorithm to the noise effect. For this study, we generated a synthetic BOLD signal (see Fig. 4) by solving the HDM (2) using the values of the biophysiological parameters $\vec{\theta}^*$ reported in Table I in the case of a single stimulus. The values of $\vec{\theta}$ were selected from the experimental values reported in Figs. 7-8 of [14]. The values of the control function characteristics $\vec{p}^*$ are reported in Table II. The intensity of the considered stimulus is $a = 0.25$. This intensity corresponds to a 25% increase in brain activity [4]. The noise-free synthetic BOLD signal was computed over a 72-second period to mimic the real data obtained from the finger-tapping experiment (see Section 4.3). Furthermore, since in practice the BOLD signal is measured at discrete times, we used 181 values measured every 0.4 seconds, to which four different levels of white noise were added to include possible errors in the measurements (see Fig. 6).

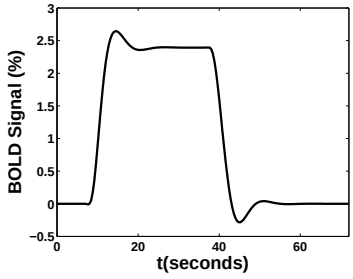

Figure 4. Noise-free synthetic BOLD signal generated using the biophysiological parameter values $\vec{\theta}^*$ in Table I. Case of a single stimulus with intensity $a = 0.25$ and control function characteristics $\vec{p}^*$ listed in Table II.

Parameter	θ_1^{-1}	θ_2	θ_3	θ_4	θ_5	θ_6	θ_7
Target ($\vec{\theta}^*$)	0.34	0.54	0.65	0.38	0.98	0.64	0.04
Initial Guess ($\vec{\theta}^{(0)}$)	0.5	0.5	0.5	0.5	0.5	0.5	0.5

Table I. Biophysiological Parameters: target vs. initial values.

We first report in Figure 5 the results obtained in the noise-free situation, i.e., both the measured BOLD signal $\vec{y}$ and the initial state vector $\vec{x}_0$ are noise-free. A noise-free initial state vector indicates that the brain is initially fully at rest. The results in Figure 5 indicate the following:

Parameter	$\widehat{T}_{\text{on}}$	$\widehat{T}_{\text{off}}$
Target ($\vec{p}^{*}$)	7	37
Initial Guess ($\vec{p}^{(0)}$)	10	30

Table II. Control Function Characteristics: target vs. initial values. Case of a single stimulus.

- The residual drops from above 500% to below 0.1% in 13 steps (see Fig. 5 (a)), which illustrates the fast convergence of the algorithm in the absence of noise. The algorithm takes less than 5 seconds to converge in this case.
- At convergence, the algorithm delivers the biophysiological parameters with a relative error of about 3% at convergence, from an initial relative error of 47%.
- At convergence, the control input parameters $\vec{p} = (\hat{T}_{\text{on}}, \hat{T}_{\text{off}})$ are obtained with a relative error of about 0.3% from an initial relative error of 20%.

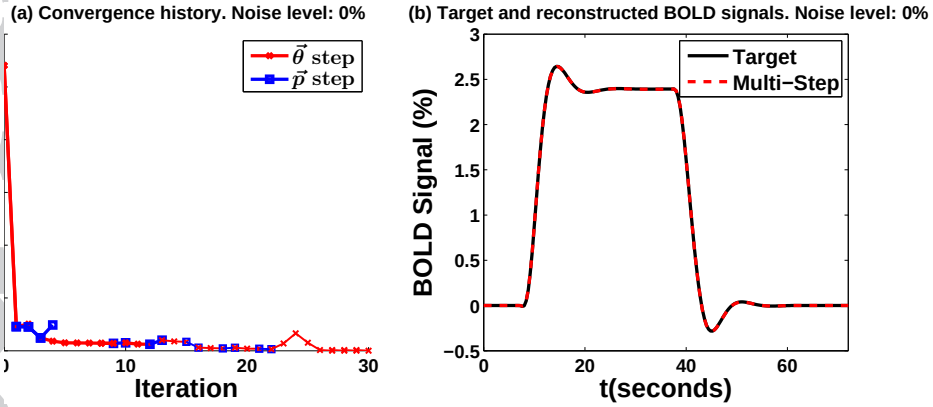

Figure 5. (a) Convergence history of the Multi-Step method. A blue line between iterations means that $\vec{p}$ was updated, whereas a red line indicates that $\vec{\theta}$ was updated. (b) Target BOLD signal (solid-black) vs. reconstructed BOLD signal (dashed-red). Case of 181 nois-free BOLD signal measurements corresponding to the biophysiological parameter values $\vec{\theta}^{*}$ in Table I and a single stimulus with characterstics listed in Table II.

Next, we present in Figs. 7-8 and Table III the results corresponding to four white noise levels, ranging from low and medium (5%, 10%) to high and very high (20%, 30%). Moreover, in all four experiments, the initial state vector, $\vec{x}_0$, was tainted with 5% white noise to mimic the situation where the brain is not fully at rest. The following observations are noteworthy:

- The initial guess for the parameter values (see Tables I and II) has been selected outside the pre-asymptotic convergence region, ensuring that the algorithm is blind to the target values of the parameters. Indeed, the initial relative errors on $\vec{\theta}$ and $\vec{p}$ are 52% and 20%, respectively. These values lead to a computed BOLD signal with a relative error that exceeds 500% for each of the four noise levels (see Fig. 7).
- The proposed computational methodology converges to the noise levels, as shown in Fig. 7. Moreover, the algorithm exhibits fast convergence since it requires few iterations to reach the noise levels. Indeed, even in the extreme case of 30% white noise on the BOLD signal

measurements, the relative residual drops from about 500% (initial residual) to the noise level after only 3 steps. Observe that steps 1 and 2 require one iteration each, while Step 3 requires two iterations. Hence, the algorithm requires a total of 4 iterations to converge (see Fig. 7 (d)). This clearly demonstrates the robustness and the efficiency of the algorithm to the noise effect.

- The algorithm delivers a highly accurate BOLD signal, as illustrated in Fig. 8. More specifically, in the extreme case of 30% white noise, the relative error on the computed BOLD signal drops from over 500% (initial error) to about 3% at convergence, after a total of 4 iterations (see Fig. 8 (d)). This appears to be an excellent accuracy level considering the relatively high noise level (30% on $\vec{y}$ and 5% on $\vec{x}_0$).
- The biophysiological parameters $\vec{\theta}$ are estimated within the range of the noise levels. For example, in the case of 30% white noise on the BOLD signal measurements (and 5% white noise on $\vec{x}_0$), the values of the biophysiological parameters are computed with a relative error of about 31% (see Table III). More importantly, the corresponding BOLD signal is highly accurate, as indicated above. This apparent discrepancy between the accuracy of the parameter estimation and its corresponding BOLD signal is due to the fact that some parameters' effects are redundant, i.e., different sets of parameters can provide identical BOLD signals. For example, as reported in [15], the effects of increasing θ_1 can be compensated by decreasing θ_2, to produce exactly the same output. On the other hand, unlike the biophysiological parameters, $\vec{\theta}$, the control input parameters $\vec{p}$ are estimated with a relative error of about 0.1% (see Table III), which is an impressive accuracy level considering the high noise level in the data.
- Figure 8 and Table III clearly demonstrate that the proposed strategy outperforms the standard TNM-CKF method proposed in [21] when estimating the biophysiological and the control input parameters together. Indeed, Figure 8 shows that the standard TNM-CKF algorithm fails dramatically to deliver a physiologically reasonable BOLD signal reconstruction. For example, in the case of 30% white noise, TNM-CKF not only requires 33 iterations to converge, but the algorithm delivers the biophysiological and control input parameters with a relative error of 104% and 22%, respectively. This inaccurate estimation leads to a very poor BOLD signal reconstruction, with multiple peaks and troughs that are inconsistent with the prototypical BOLD regime, as depicted in Fig. 8 (d).

4.1.2. Sensitivity to the number of BOLD signal measurements. The goal here is to examine the effect of the number of measurements on the accuracy of the proposed method. To this end, the synthetic BOLD signal measurements were generated using the biophysiological parameters listed in Table I and the control input parameters listed in Table IV. In this experiment, we have set the start and end times of the stimulus, $T_{\text{on}} = 0s$, $T_{\text{off}} = 0.5s$, and we assumed that the intensity of the

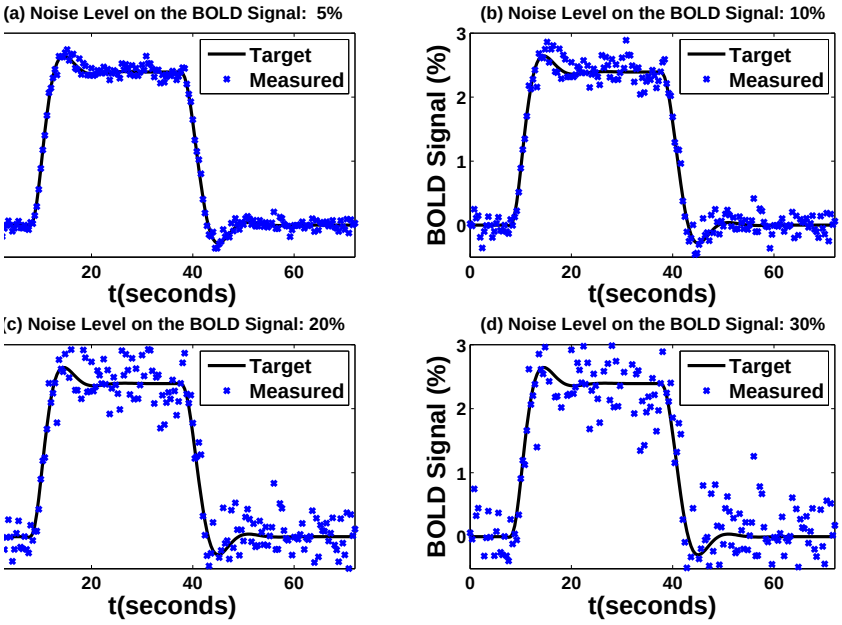

Figure 6. Target BOLD signal (solid-black) vs. 181 noisy BOLD signal measurements (dots-blue) corresponding to the biophysiological parameter values $\vec{\theta}^*$ in Table I. Case of a single stimulus with characterstics listed in Table II.

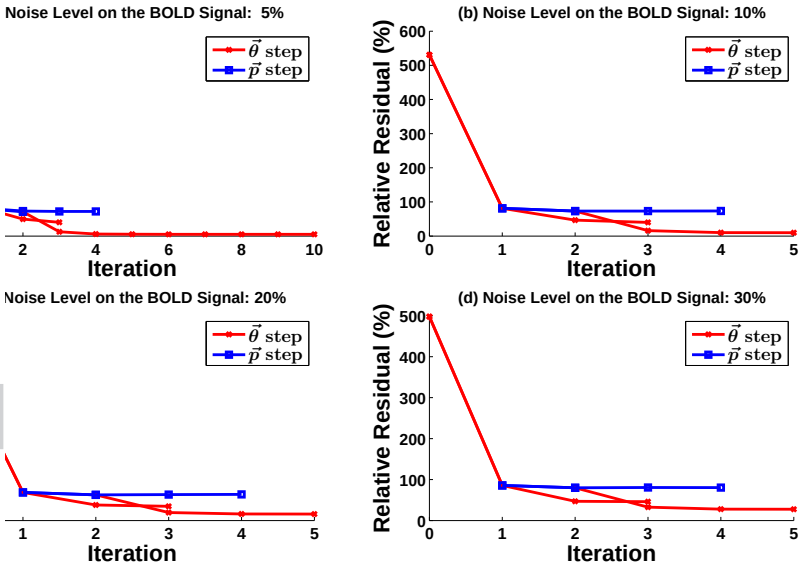

Figure 7. Convergence history of the Multi-Step method. Case of 181 BOLD signal measurements, 5% white noise on the initial state vector $\vec{x}_0$, and a single stimulus. A blue line between iterations means that $\vec{p}$ was updated; a red line indicates that $\vec{\theta}$ was updated.

stimulus, a, and the delay time between the stimulus and the neural activity, δ_t (see Equation 2), are to be determined, i.e., $\vec{p} = (\widehat{T}_{\text{on}}, a)^T$ (see Equation 1), along with the biophysiological parameters $\vec{\theta}$. The synthetic BOLD signal was generated over a 32-second period as a mock-up of the real data employed in the experiment in Section 4.4. This signal was then sampled using several different time steps to assess the effect of the number of measurements. We present the results obtained for

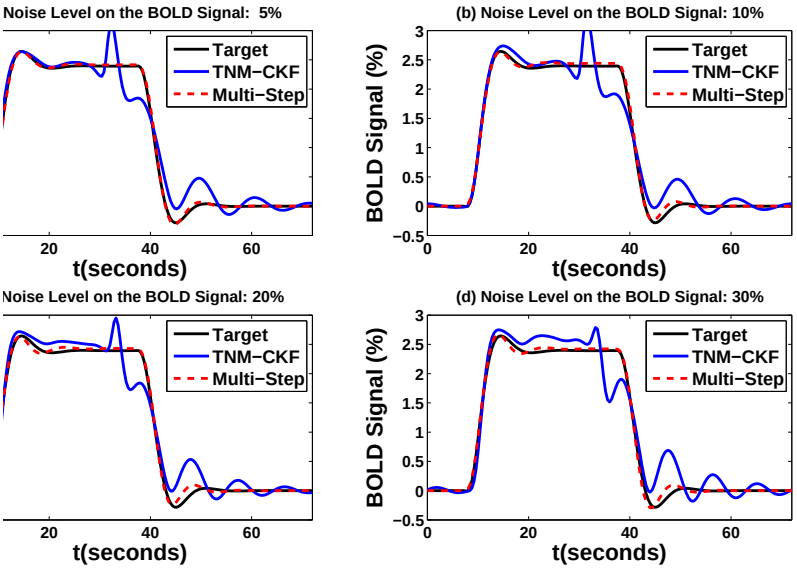

Figure 8. Target BOLD signal (solid-black) vs. reconstructed BOLD signals using Multi-Step method (dashed-red) and the standard TNM-CKF approach (solid-blue). Case of 181noisy BOLD signal measurements, 5% white noise on the initial state vector $\vec{x}_0$, and a single stimulus.

	Multi-Step	TNM-CKF
$\frac{\|\vec{\theta}^* - \vec{\theta}^{(comp)}\|_2}{\|\vec{\theta}^*\|_2}$	31%	104%
$\frac{\|\vec{p}^* - \vec{p}^{(comp)}\|_2}{\|\vec{p}^*\|_2}$	0.1%	22%

Table III. Relative errors on the computed parameter values: Multi-Step strategy vs. standard TNM-CKF approach. Case of 30% white noise on 181 BOLD signal measurements, 5% white noise on the initial state vector $\vec{x}_0$, and a single stimulus.

BOLD signals measured with: (a) 13 data points, i.e., $\Delta t = 8/3$ s and $\vec{y} \in \mathbb{R}^{13}$; (b) 17 data points, i.e., $\Delta t = 2s$ and $\vec{y} \in \mathbb{R}^{17}$; (c) 33 data points, i.e., $\Delta t = 1s$ and $\vec{y} \in \mathbb{R}^{33}$; (d) 65 data points, i.e., $\Delta t = 0.5s$ and $\vec{y} \in \mathbb{R}^{65}$; and (e) 129 data points, i.e., $\Delta t = 0.25s$ and $\vec{y} \in \mathbb{R}^{129}$. In addition, 30% white noise was added to each set of measurements (see Fig. 9). We solved the inverse problem 6 using each of the considered four sets of synthetic BOLD signal measurements, successively. The results are reported in Figs. 10-11. The following remarks are worth noting:

- Fig. 10 indicates that, as expected, the performance of the proposed algorithm tends to either improve or deteriorate depending on the number of BOLD signal measurements. More specifically, this experiment reveals that the minimum number of measurements needed for the algorithm to converge is 13. Using less data points results in a measured BOLD signal that does not exhibit the impulse response and post-stimulus undershoot of the true BOLD signal, i.e, the BOLD signal measurements do not reflect the underlying neuronal activity which drives the BOLD response. Therefore, it is not surprising for the algorithm not to converge. Although the algorithm converges using 13 data points, the computed BOLD signal has a relative error

above 30%, which is still not an acceptable accuracy level. There is a significant improvement in the accuracy of the computed BOLD signal when the number of data points is increased to 17. Indeed, the relative error drops to 16% (see Fig. 11 (a)-(b)). This relative error with 17 data points seems to be acceptable given the high noise level on the data. Doubling the number of data points from 33 to 65 measurements reduces the relative error on the computed BOLD signal by a factor of 2. Indeed, the relative error drops from about 16% to 8% (see Fig. 11 (c)-(d)). Observe that Fig. 10 indicates the presence of a plateau-type convergence when the number of measurements is greater than 65. Indeed, the relative error drops minimally from 8% to only 6% in spite of increasing the number of data points by a factor of two (from 65 to 129). This suggests that there is no significant gain in increasing the number of measurements.

- There is a significant accuracy improvement in the parameter estimation, particularly for $\vec{p}$, as the number of measurements increases. Indeed, the accuracy of the estimated values of $\vec{\theta}$ improves by a factor of 2 (from 46% to 23% relative error) when the number of data points is increased from 17 to 65, whereas the accuracy of the estimated values of $\vec{p}$ improves by a factor of 5 (from 46% to 9% relative error). Note that the improvement in the accuracy also tends to stagnate, which is consistent with the results in the reconstruction of the BOLD signal.
- The relative error on the BOLD signal in the case of 33 measurements is almost equal to that in the case of 17 measurements, which is contrary to the overall trend. However, a closer look at Fig. 11 indicates that the computed BOLD signal with 33 measurements (Fig. 11 (c)) is more physiologically plausible than the one with 17 measurements (Fig. 11 (b)). Specifically, the reconstructed BOLD signal with 17 data points exhibits a more pronounced but shorter-lasting post-stimulus undershoot that is not in agreement with the target BOLD signal, as well as a second undershoot after the brain should have returned to its resting state (see Fig. 11 (b)).

In summary, this experiment suggests that, as a possible practical guideline, the minimum number of BOLD signal measurements should be in the range 17–33 in order to achieve both convergence and an acceptable accuracy level on the reconstructed BOLD signal. These measurement guidelines appear to be of practical interest, as illustrated by the numerical experiments with real data (see Sections 4.3-4.4). Indeed, the BOLD signal was measured 25 times in the finger-tapping experiment (Section 4.3) and 16 times in the face repetition experiment (Section 4.4). Note that this experiment has been performed in the case where the BOLD signal is tainted with 30% white noise, an extreme scenario. Therefore, using this rule in the presence of lower noise levels in the measurements is expected to lead to more accurate results.

Figure 9. Target BOLD signal (solid-black) and noisy BOLD signal measurements(dots-blue). Case of a single stimulus and 30% white noise on the measured BOLD signal.

Parameter	$\widehat{T}_{\text{on}}$	a
Target ($\vec{p}^{*}$)	0.2	0.3
Initial Guess ($\vec{p}^{(0)}$)	0.5	0.35

Table IV. Control Function Characteristics: target vs. initial values

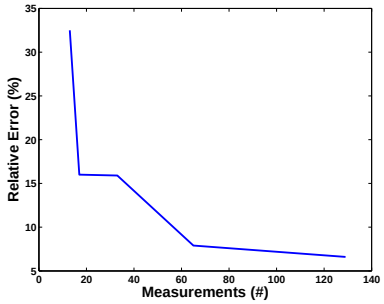

Figure 10. Relative error on the BOLD signal vs. number of measurements. Case of a single stimulus and 30% white noise on the measured BOLD signal.

4.2. *Experiment 2: Synthetic data corresponding to multiple brain activation stimuli*

Next, we present the results of the model calibration using synthetic BOLD signal measurements corresponding to four different stimuli. Specifically, we fixed the set of biophysiological parameters (see Table I), and generated synthetic BOLD signals by considering *On-Off* stimuli (see Equation 1) which differ by their intensity values. Specifically, we consider the following intensities: 0.2, 0.3, 0.4, and 0.5. These values have been chosen because the percent change in neuronal signal is in the range 20–50% for excitatory activity during visual stimulation conditions [4, 29]. For each stimulus, we selected $T_{\text{on}} = 0s$ and $T_{\text{off}} = 0.5s$. The target BOLD signal measurements were computed with a time step $\Delta t = 0.5s$, for a total of 65 measurements over a 32-second interval. Fig. 12 shows the considered stimuli (see Fig. 12 (a)) and their corresponding noise-free BOLD signal responses, $\vec{y}_j \in \mathbb{R}^{65}$, $j = 1, ..., 4$ (see Fig. 12 (b)). Furthermore, 30% white noise was added to the 65 data points in each case, to obtain $\widetilde{\vec{y}}_j \in \mathbb{R}^{65}$ (see Fig. 13). The goal of this experiment is to estimate the biophysiological parameters $\vec{\theta}^{*}$ (see Table I) and the control input parameters $\vec{p}^{*} = (\widehat{T}^{*}_{\text{on}}, a^{*})^{T}$ (see Table V) using the four sets of synthetic BOLD signal measurements, $\widetilde{\vec{y}}_j$, depicted in Fig. 13. To this end, the proposed algorithm delivered, for each set of measurements $\widetilde{\vec{y}}_j$, a set of biophysiological parameters, $\vec{\theta}_j$, whose values are listed in Table VI. Then, we averaged $\vec{\theta}_j$ to obtain the sought-after biophysiological parameter values, $\vec{\theta}_{\text{avg}}$ (see Table VI). Next, we applied the proposed algorithm, this time with $\vec{\theta} = \vec{\theta}_{\text{avg}}$ and using the noisy synthetic BOLD signal measurements $\vec{y}_j$ to estimate $\vec{p}_j = (\widehat{T}_{\text{on},j}, a_j)^{T}$. The final computed values of the control function parameters are $\vec{p}_{j,\text{avg}} = (\widehat{T}_{\text{on,avg}}, a_j)^{T}$, where $\widehat{T}_{\text{on,avg}}$ is the averaged value of the computed $\widehat{T}_{\text{on},j}$ (see TableVIII). Finally, the computed parameters $(\vec{\theta}_{\text{avg}}, \vec{p}_{j,\text{avg}})$ were used to construct the BOLD signals depicted in Fig. 16. The following observations are noteworthy:

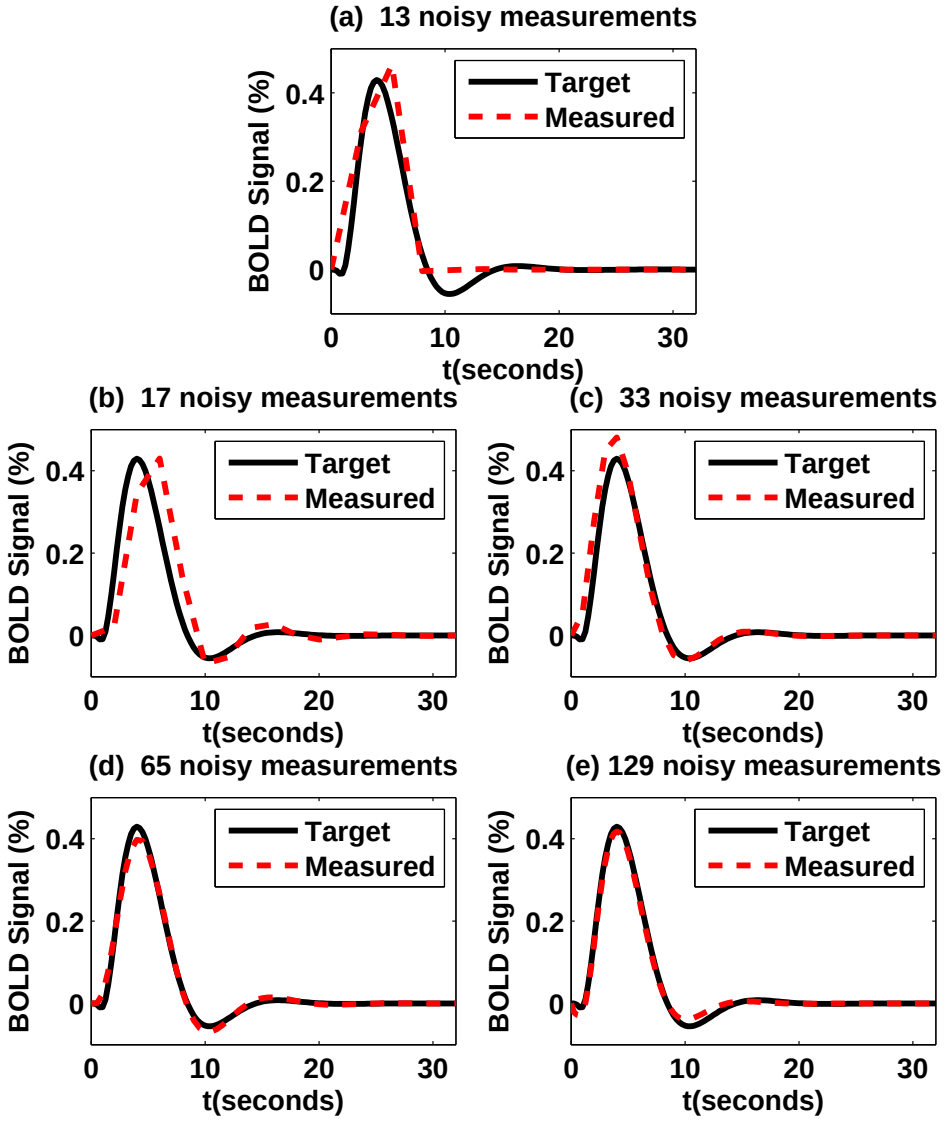

Figure 11. Effect of the number of BOLD signal measurements: Target BOLD signal (solid-black) vs. reconstructed BOLD signal using Multi-Step method (dashed-red). Case of a single stimulus and 30% white noise on the measured BOLD signal.

- The proposed computational methodology very quickly converges to the noise level, both for estimating $\vec{\theta}_{\text{avg}}$ (see Fig. 14), and evaluating $\vec{p}_{j,\text{avg}}$ (see Fig. 15). Indeed, for the four considered intensities, the relative residual drops from 900% to 30% in only two steps, after a total of 4-5 iterations. This again demonstrates the robustness and the efficiency of the algorithm to the noise effect.
- The proposed strategy for estimating the sought-after biophysiological parameters by averaging the computed values for each set of BOLD signal measurements is proven to be an effective approach. Indeed, for each stimulus, the reconstructed BOLD signal is obtained

with a relative error below 10% (see Fig. 16). This appears to be an excellent accuracy level, given the very high noise level (30%) in the BOLD signal measurements.

- The computed values of the biophysiological parameters, which have been obtained by averaging the computed values from the four different stimuli, yields $\vec{\theta}_{\text{avg}}$ with a relative error of about 23%, and six of the seven computed biophysiological parameters are obtained with relative errors below the noise level (see Table VI). Note that, similarly to Experiment 1, the corresponding BOLD signals are computed with a high accuracy level. We also observe the apparent "redundancy" in the values of the biophysiological parameters, that is, even with a low accuracy level on some of the biophysiological parameters (e.g., θ_1) the BOLD signal is still reconstructed with a high accuracy level.
- The multi-stage algorithm is able to distinguish the different levels of neuronal activity, an important feature, for each BOLD response. Indeed, the model calibration delivers the control input parameters with an excellent level of accuracy, as reported in Table VII. For all four stimuli, the relative error on the computed parameters is below 3%. In addition, Table VIII indicates that $\widehat{T}_{\text{on}}$ is computed with a relative error of 8.5%.

	Target ($\vec{p}^*$)	
	$\widehat{T}_{\text{on}}$	a
Stimulus A	0.2	0.2
Stimulus B	0.2	0.3
Stimulus C	0.2	0.4
Stimulus D	0.2	0.5

Table V. Control Function Characteristics: Target values corresponding to the four stimuli used in Experiment 2.

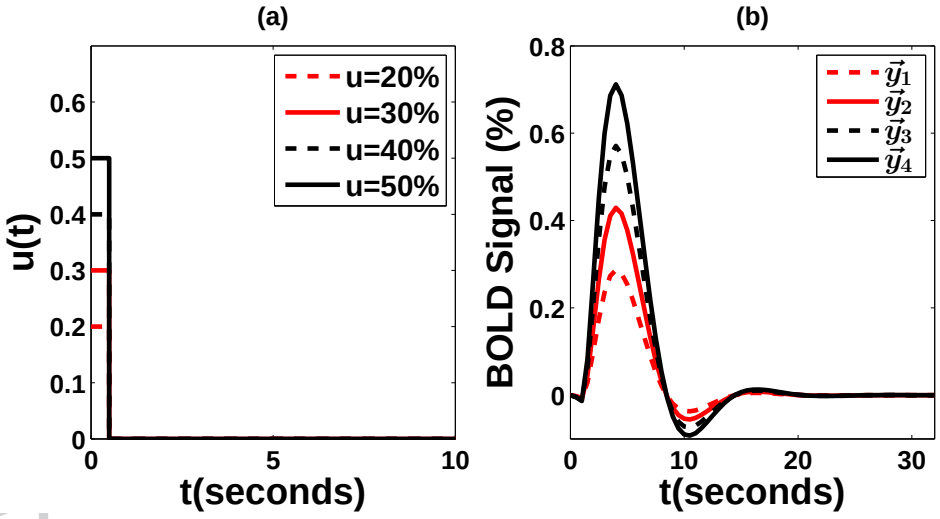

Figure 12. (a) On-Off stimuli corresponding to four intensity levels and (b) their corresponding noise-free synthetic BOLD signal responses, computed using the values of $\vec{\theta}^*$ listed in Table I, $T_{\text{on}} = 0s$, and $T_{\text{off}} = 0.5s$.

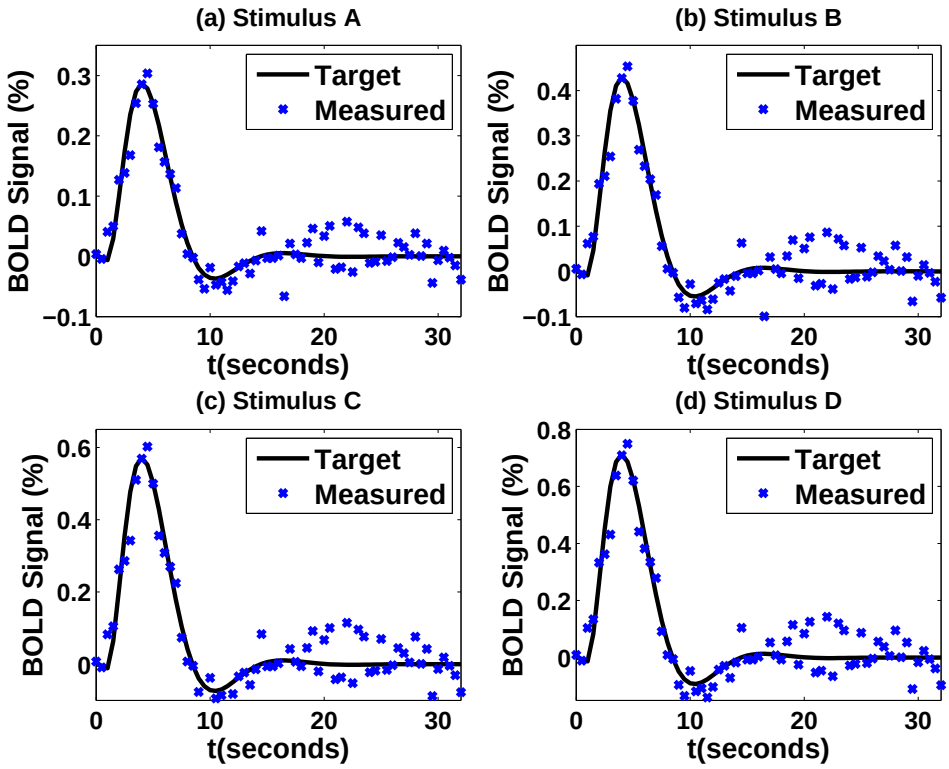

Figure 13. Target BOLD signal (solid-black) vs. measured synthetic BOLD signal tainted with 30% white noise (dots-blue), Experiment 2: case of multiple stimuli corresponding to four different intensities listed in Table V.

Parameter	θ_1^{-1}	θ_2	θ_3	θ_4	θ_5	θ_6	θ_7
Target ($\vec{\theta}^*$)	0.34	0.54	0.65	0.38	0.98	0.64	0.04
Stimulus A ($\vec{\theta}_1$)	0.54	0.61	0.55	0.41	0.72	0.52	0.02
Stimulus B ($\vec{\theta}_2$)	0.55	0.61	0.56	0.40	0.75	0.52	0.03
Stimulus C ($\vec{\theta}_3$)	0.54	0.59	0.57	0.40	0.79	0.49	0.03
Stimulus D ($\vec{\theta}_4$)	0.54	0.58	0.57	0.40	0.78	0.47	0.04
Averaged ($\vec{\theta}_{\text{avg}}$)	0.542	0.599	0.560	0.402	0.759	0.500	0.033
$\frac{\lvert\theta_i^* - \theta_{\text{avg},i}\rvert}{\lvert\theta_i^*\rvert}$	59%	11%	14%	6%	23%	22%	18%

Table VI. Biophysiological Parameters: target vs. computed values. Case of 30% white noise on the synthetic BOLD signal measurements, and four stimuli corresponding to four different intensities.

		a	Relative Error
Stimulus A	Target	0.2	0.5%
	Computed	0.199	
Stimulus B	Target	0.3	0.3%
	Computed	0.299	
Stimulus C	Target	0.4	2.3%
	Computed	0.391	
Stimulus D	Target	0.5	2.2%
	Computed	0.489	

Table VII. Stimulus Intensity: target vs. computed values. Case of 30% white noise on the synthetic BOLD signal measurements, and four stimuli corresponding to four different intensities.

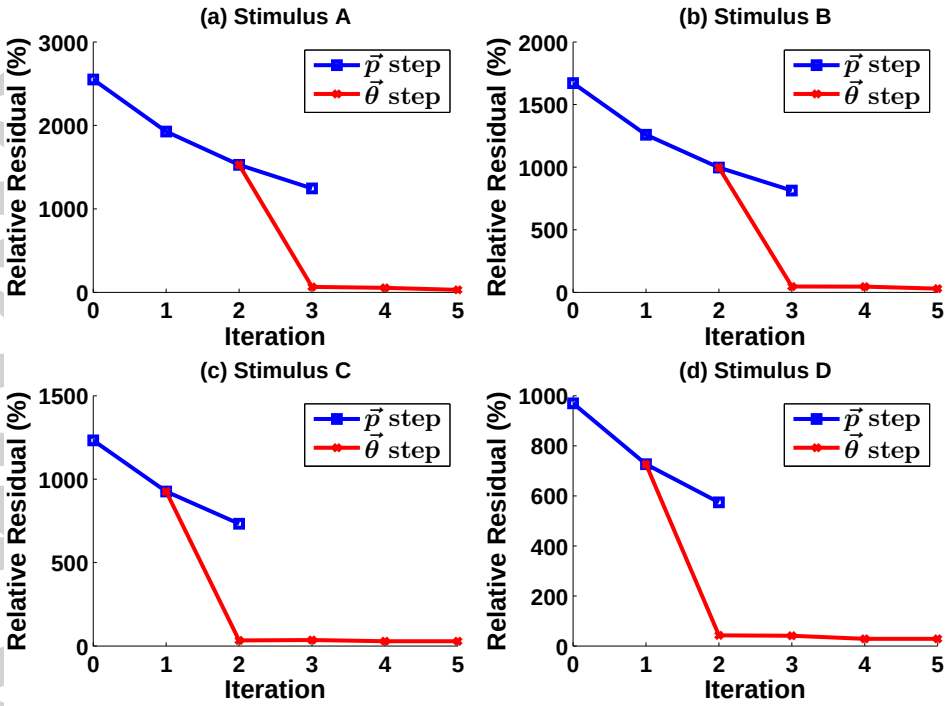

Figure 14. Convergence history of the Multi-Step method to estimate $\vec{\theta}_{\text{avg}}$. Case of 65 synthetic BOLD signal measurements tainted with 30% white noise, and four different stimuli. A blue line between iterations means that $\vec{p}$ was updated; a red line indicates that $\vec{\theta}$ was updated.

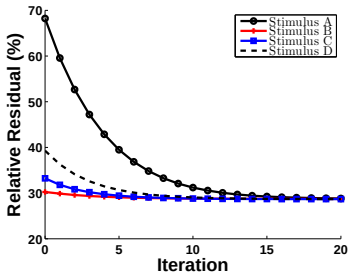

Figure 15. Convergence history of the Multi-Step algorithm to estimate $\vec{p}_{j,\text{avg}} = (\widehat{T}_{\text{on,avg}}, a)^T$ using $\vec{\theta}_{\text{avg}}$ and the four sets of synthetic BOLD signal measurements.

Parameters	$\widehat{T}_{\text{on}}$
Target	0.2
Initial Guess	0.5
Stimulus A ($\widehat{T}_{\text{on},1}$)	0.219
Stimulus B ($\widehat{T}_{\text{on},2}$)	0.217
Stimulus C ($\widehat{T}_{\text{on},3}$)	0.218
Stimulus D ($\widehat{T}_{\text{on},4}$)	0.216
$\widehat{T}_{\text{on,avg}}$	0.217
$\dfrac{\lvert\widehat{T}_{\text{on}^*} - \widehat{T}_{\text{on,avg}}\rvert}{\lvert\widehat{T}_{\text{on}^*}\rvert}$	8.5%

Table VIII. Control Function Characteristics: target, initial, and computed values. Case of an *On-Off* stimulus with four different intensities.

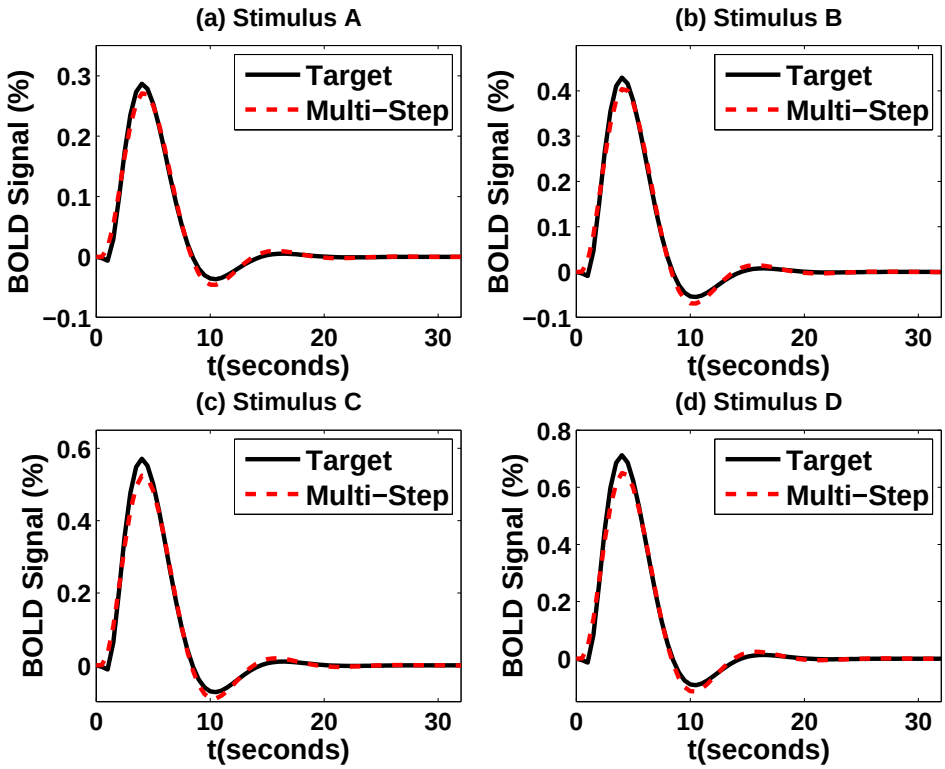

Figure 16. Target synthetic BOLD signal (solid-black) vs. reconstructed BOLD signal using the Multi-Step method (dashed-red), Experiment 2: case of four stimuli and 30% white noise on the synthetic BOLD signal measurements.

4.3. Experiment 3: Real data corresponding to a finger-tapping experiment

Here, we investigate the performance of the proposed solution methodology when using real BOLD signal measurements corresponding to a single stimulus. The considered data were obtained from an fMRI scan of a male subject instructed to complete a finger-tapping task in a study approved by the Institutional Review Board at Nationwide Children's Hospital in Columbus, Ohio. In this experiment, head motion was restricted by firm cushions packed around the head, and by use of a head strap. The final data were taken with $\Delta t = 3s$ over a 72-second interval, providing a total of 25 measurements, that is, $\widetilde{\vec{y}} \in \mathbb{R}^{25}$ [23]. The goal of this experiment is to apply the proposed algorithm using the real BOLD signal measurements, $\widetilde{\vec{y}}$, to estimate $\vec{\theta}$ and $\vec{p} = (\widehat{T}_{\text{on}}, \widehat{T}_{\text{off}})^T$. Due to the lack of a priori knowledge of the parameters' values, we used the initial guesses $\vec{\theta}^{(0)}$ and $\vec{p}^{(0)}$ given in Tables I and II, respectively. We assumed, however, that the intensity of the stimulus was $a = 0.2$, which corresponds to a 20% increase in neuronal activity. This appears to be a reasonable estimation given the relatively mild nature of the considered stimulus [4,29]. The results of this numerical experiment are reported in Fig. 17 and Tables IX-X. These results suggest the following:

- Fig. 17 (a) illustrates the convergence efficiency of the proposed algorithm. Indeed, the relative residual decreased from about 400% to 4.7% after 3 steps, totaling 10 iterations only.

- The computed BOLD signal appears to be very accurate (see Fig. 17 (b)). With a relative residual of 4.7%, the computed BOLD signal exhibits the canonical brief overshoot and post-stimulus undershoot that are clearly in agreement with the measured signal.
- The computed parameter values reported in Table IX appear to be physiologically plausible [3]. These values fall within the range of the experimental values obtained in [14].

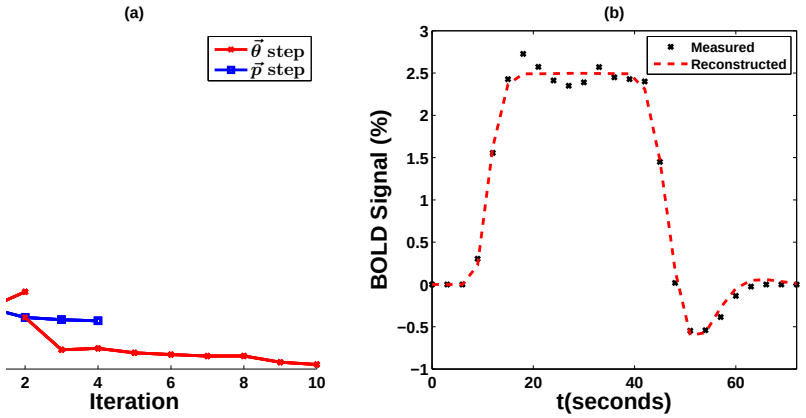

Figure 17. (a) Convergence history using real fMRI measurements corresponding to a finger-tapping experiment. (b) Computed BOLD signal after 6 steps (dashed-red) vs. real fMRI measurements (25 data points, dots-black).

Parameter	θ_1^{-1}	θ_2	θ_3	θ_4	θ_5	θ_6	θ_7
Computed Value	0.99	0.53	0.36	0.09	0.58	0.28	0.06

Table IX. Biophysiological Parameters: computed values, finger-tapping experiment.

Parameter	$\widehat{T}_{\text{on}}$	$\widehat{T}_{\text{off}}$
Computed Value	7.23	36.98

Table X. Control Function Characteristics: computed values, finger-tapping experiment.

4.4. Experiment 4: Real data corresponding to a face repetition experiment

Here, we assess the performance of the proposed computational strategy when using real BOLD signal measurements corresponding to multiple stimuli. We consider the open-access data taken from a repetition priming experiment [28]. In this experiment, the subject was asked to make fame judgements by making a key press. The subject was exposed to both famous and nonfamous faces, and each face was repeated, for a total of four distinct events: Famous1, Famous2, Nonfamous1, and Nonfamous2. The data were averaged over 26 occurrences of each event, with $T_{\text{on}} = 0s$, $T_{\text{off}} = 0.5s$. Hence, for each event, we have 16 averaged data points, that is, $\widetilde{\vec{y}}_j \in \mathbb{R}^{16}$, $j = 1, \ldots, 4$ (see Fig. 20). We applied the proposed algorithm as described in Section 4.2. Specifically, since we have no knowledge about the sought-after parameter values, we used the initial guesses given in Tables I and IV to calibrate the model for each of the four stimuli. For each set of measurements $\widetilde{\vec{y}}_j$, the

proposed algorithm delivered a set of biophysiological parameters, $\vec{\theta}_j$. We then averaged $\vec{\theta}_j$ to obtain the sought-after biophysiological parameter values, $\vec{\theta}_{\text{avg}}$ (see Table XI). Furthermore, we applied the proposed algorithm, this time using $\vec{\theta}_{\text{avg}}$ and the real BOLD signal measurements $\widetilde{\vec{y}}_j$ to estimate $\vec{p}_j = (\widehat{T}_{\text{on},j}, a_j)^T$. The obtained control function parameters are $\vec{p}_{j,\text{avg}} = (\widehat{T}_{\text{on,avg}}, a_j)^T$, where $\widehat{T}_{\text{on,avg}}$ is the averaged value of the computed $\widehat{T}_{\text{on},j}$. Finally, the computed parameters $(\vec{\theta}_{\text{avg}}, \vec{p}_{j,\text{avg}})$ were used to construct the BOLD signals depicted in Fig. 20. The obtained results depicted in Figs. 18-20 and Tables XI-XII indicate the following:

- The algorithm exhibits fast convergence when estimating both $\vec{\theta}_{\text{avg}}$ (see Fig. 18) and $\vec{p}$ (see Fig. 19). Indeed, the relative residual reaches its asymptotic regime in one step (and no more than 5 iterations) for each stimulus. Observe that these results indicate that the biophysiological parameters were not updated when estimating $\vec{\theta}_{\text{avg}}$.
- The reconstructed BOLD signals depicted in Fig. 20 have residuals ranging from 23% to 36%, relative to the averaged data. While this may appear to be a high residual, note that the reconstructed BOLD signals overall fall within the range of the measurements. We must keep in mind that, although each set of measured data is averaged over 26 instances of the associated event, the data are still highly noisy, as demonstrated by the large error bars associated with each of the measurements.
- The computed BOLD signal is overall in agreement with the measured data, and seems to be even more physiologically plausible than the noisy measurements. Indeed, one can observe in Fig. 20 (b), for example, that the averaged data show a negative BOLD response at a time when the activity should already have returned to its corresponding baseline. In addition, the computed values given in Tables XI-XII along with the computed value $\widehat{T}_{\text{on,avg}} = 0.556$ s are both physiologically plausible and consistent with the data, that is, the first appearance of a famous face causes the largest change in neuronal activity, followed by the first appearance of a nonfamous face, while the repetition of the events causes a smaller reaction than the first appearance.

Parameter	θ_1^{-1}	θ_2	θ_3	θ_4	θ_5	θ_6	θ_7
$\vec{\theta}_{\text{avg}}$	0.618	0.283	0.703	0.343	0.826	0.386	0.337

Table XI. Biophysiological Parameters: Computed values for the face repetition experiment.

Event	Computed Stimulus Intensity (a)
Famous1	0.40
Famous2	0.33
Nonfamous1	0.38
Nonfamous2	0.31

Table XII. Control Input Parameters: Computed values for the face repetition experiment.

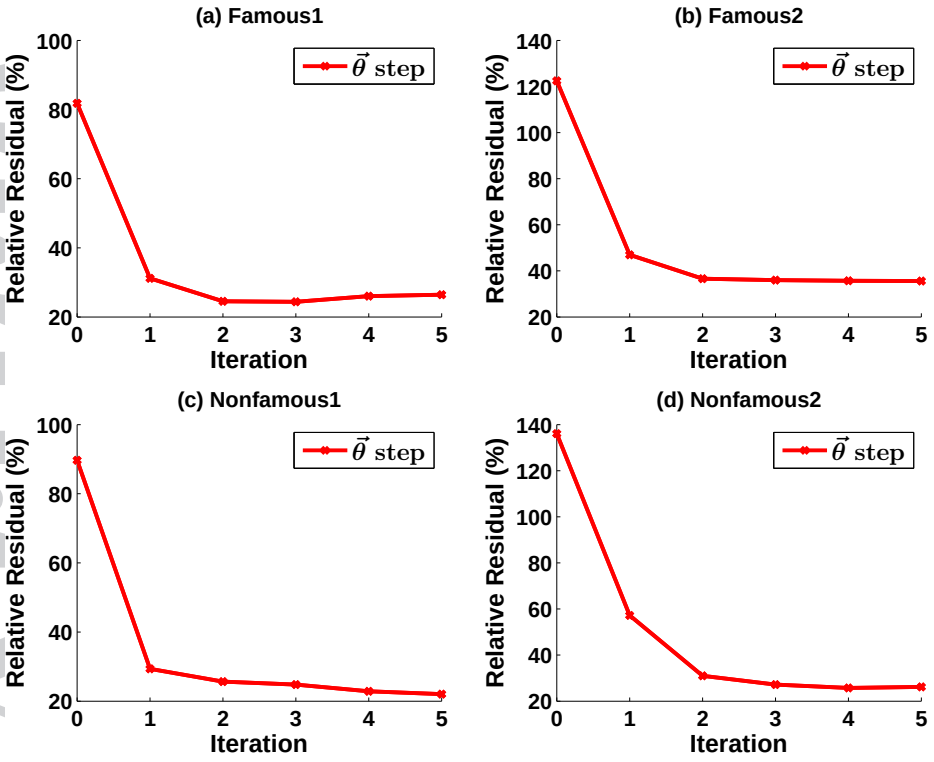

Figure 18. Convergence history of the Multi-Step method to estimate $\vec{\theta}_{\text{avg}}$. Case of face repetition measurements. The algorithm converges in one step, i.e., only $\vec{\theta}$ was updated.

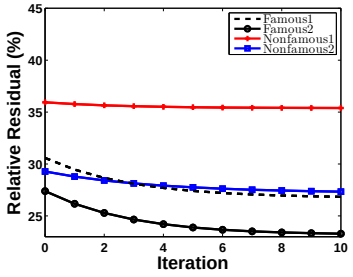

Figure 19. Convergence History of the Multi-Step Algorithm: Using $\vec{\theta}_{\text{avg}}$ to estimate $\vec{p}_{j,\text{avg}} = (\widehat{T}_{\text{on,avg}}, a)^T$ for four face repetition events.

5. SUMMARY AND CONCLUSION

We have investigated numerically the problem of simultaneously estimating the biophysiological parameters of the hemodynamic model and the external stimulus characteristics from the knowledge of some BOLD signal measurements. We have proposed an efficient solution methodology to estimate the biophysiological parameters and the external stimulus characteristics to fit the BOLD signal output of the hemodynamic model. This technique is a multi-stage strategy which estimates successively each set of parameters by using the standard TNM-CKF method in a prediction/correction-type approach. The defining features of this method are its ability to perform

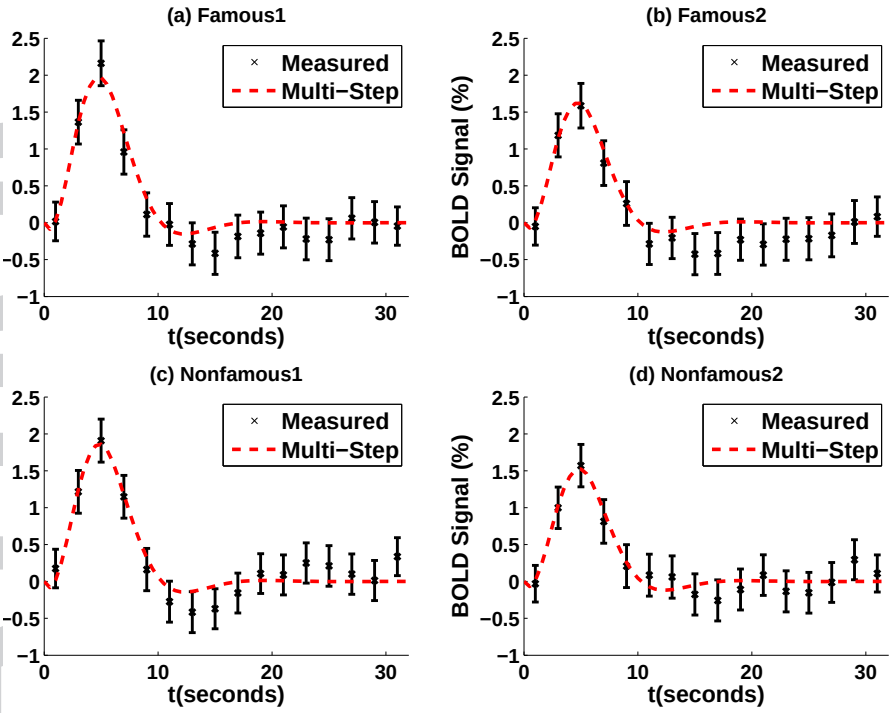

Figure 20. Averaged fMRI measurements (black) vs. reconstructed BOLD signal using Multi-Step method (dashed-red) for the face repetition experiment.

without a priori knowledge on the parameter values, as well as its ability to retrieve both the biophysiological parameters and the external stimulus characteristics. The strategy is also capable of characterizing different levels of neural activity in a single subject, which appears to be a distinguished, powerful feature. The presented numerical results illustrate the robustness and efficiency of the proposed method. This new method has successfully calibrated the hemodynamic model using data from actual fMRI images. Furthermore, the algorithm is cost effective. It can be run on any personal desktop or laptop machine, and requires only few seconds to perform a single calibration.

ACKNOWLEDGEMENTS

The authors would like to thank the anonymous referee for his/her very valuable remarks and suggestions.

APPENDIX A. TNM-CKF ALGORITHM DESCRIPTION

The goal here is to provide a succinct presentation of the standard TNM-CKF algorithm for self-containment purposes, only. A detailed description of the algorithm can be found in [21]. This algorithm is based on two coupled procedures: a Tikhonov-regularized Newton Method (TNM) and a Cubature Kalman Filter (CKF). Here, we describe the algorithm for a single event.

5.1. The Tikhonov-regularized Newton Method.

This procedure is employed to address both the nonlinearity and the stability issues of the inverse problem 6. At iteration m, the standard TNM method requires solving the following linear system:

$$\left(J_B^{T(m)} J_B^{(m)} + \mu I\right) \delta\vec{z}^{(m)} = J_B^{T(m)} \left(\tilde{y} - y^{(m)}\right) \tag{15}$$

and updating

$$\vec{z}^{(m+1)} = \vec{z}^{(m)} + \delta\vec{z}^{(m)} \tag{16}$$

for the next iteration. J_B is the Jacobian matrix of the BOLD signal 4, given by:

$$[J_B]_{i,j} = \frac{\partial B}{\partial z_j}\left(\vec{\theta}^{(m)}, \vec{p}^{(m)}; \vec{x}^{(m)}(t_i)\right) \tag{17}$$

for $i = 1, 2, \ldots, N_m$, $j = 1, 2, \ldots, N_z^{(m)}$. I is the identity matrix and μ is the Tikhonov regularization parameter, whose value is selected using a trial and error procedure. $\vec{z}$ is the target parameters vector ($\vec{z} = \vec{\theta}$ or $\vec{z} = \vec{p}$). $N_z^{(m)}$ represents the size of $\vec{z}$ at iteration m ($N_z^{(m)} = 7$ if $\vec{z} = \vec{\theta}$, $N_z^{(m)} = 2$ if $\vec{z} = \vec{p}$).

5.2. The Cubature Kalman Filter.

The CKF algorithm introduced in [15] is employed here to address the effect of noise in the data. CKF evaluates the BOLD signal in two steps: (i) a time update step and (ii) a measurement update step.

(i) Time Update. Here, predicted estimates of the state vector and its associated error covariance are delivered for the next time step. Assume that the state vector $\vec{x}_k$ and covariance P_k have been computed for $k = 0, 1, \ldots, t$. Then, the state vector, $\vec{x}_{t+1}$, and the covariance, P_{t+1}, for the next time step are computed by first finding predicted estimates $\widehat{\vec{x}}_{t+1}$ and $\widehat{P}_{t+1}$ as follows:

1. We begin by evaluating the cubature points,

$$\vec{c}_{i,t} = S_t\vec{\xi}_i + \vec{x}_t; \qquad i = 1, 2, \ldots, 8 \tag{18}$$

where S_t is computed by a Cholesky factorization of P_t, that is,

$$P_t = S_t S_t^T, \tag{19}$$

and $\vec{\xi}_i$ is the ith column of the cubature points matrix ξ given by:

$$\xi = \begin{bmatrix} 2 & 0 & 0 & 0 & -2 & 0 & 0 & 0 \\ 0 & 2 & 0 & 0 & 0 & -2 & 0 & 0 \\ 0 & 0 & 2 & 0 & 0 & 0 & -2 & 0 \\ 0 & 0 & 0 & 2 & 0 & 0 & 0 & -2 \end{bmatrix} \tag{20}$$

2. Next, we evaluate the process at the cubature points to obtain the propagated cubature points at time $t + 1$, which requires solving the following differential system:

$$\begin{cases} \dot{\vec{z}}_i = A\left(\vec{\theta}, \vec{p}; \vec{z}_i\right) \\ \vec{z}_{i,t} = \vec{c}_{i,t} \end{cases}; \qquad i = 1, 2, \ldots, 8, \tag{21}$$

where A is given by 3.

3. The average of the cubature points found in step 2 serves as a prediction for the state at time $t + 1$, that is,

$$\widehat{\vec{x}}_{t+1} = \frac{1}{8}\sum_{i=1}^{8} \vec{z}_{i,t+1} \tag{22}$$

4. The time update step ends with the calculation of the predicted error covariance, $\widehat{P}_{t+1}$:

$$\widehat{P}_{t+1} = \frac{1}{m}\sum_{i=1}^{8} \vec{z}_{i,t+1}\vec{z}_{i,t+1}^T - \widehat{\vec{x}}_{t+1}\widehat{\vec{x}}_{t+1}^T + Q_{t+1}, \tag{23}$$

where Q_{t+1} is the process noise covariance at time $t + 1$ defined in Chapter 2.

(ii) Measurement Update. In this step, we correct the predicted values given by 22 and 23 in order to evaluate the BOLD signal at time $t + 1$. The measurement update is performed as follows:

1. We begin by correcting $\widehat{\vec{x}}_{t+1}$ to obtain $\vec{x}_{t+1}$. To do so, we first evaluate the predicted cubature points,

$$\widehat{\vec{c}}_{i,t+1} = \widehat{S}_{t+1}\vec{\xi}_i + \widehat{\vec{x}}_{t+1}; \qquad i = 1, 2, \ldots, 8 \tag{24}$$

where $\widehat{S}_{t+1}$ is once again computed by the Cholesky factorization of $\widehat{P}_{t+1}$, that is,

$$\widehat{P}_{t+1} = \widehat{S}_{t+1}\widehat{S}_{t+1}^T. \tag{25}$$

Next, and similarly to the predicted state vector, we obtain the predicted BOLD signal at time $t+1$ by averaging the BOLD signal over the predicted cubature points 24

$$\widehat{y}_{t+1} = \frac{1}{8}\sum_{i=1}^{8} B\left(\vec{\theta}, \vec{p}; \widehat{\vec{c}}_{i,t+1}\right). \tag{26}$$

Using 22 and 26, we deduce the corrected value of $\vec{x}_{t+1}$, given by:

$$\vec{x}_{t+1} = \widehat{\vec{x}}_{t+1} + (\widetilde{y}_{t+1} - \hat{y}_{j+1})\overrightarrow{W}_{t+1}, \tag{27}$$

where $\tilde{y}_{t+1}$ is the measured BOLD signal at time $t+1$, $\overrightarrow{W}_{t+1}$ is the *Kalman gain* at time $t+1$, given by:

$$\overrightarrow{W}_{t+1} = M_{t+1}^{-1}\overrightarrow{N}_{t+1}, \tag{28}$$

with

$$M_{t+1} = \frac{1}{8}\sum_{i=1}^{8}\left(B\left(\vec{\theta}, \vec{p}; \widehat{\vec{c}}_{i,t+1}\right)\right)^2 - \widehat{y}_{t+1}^2 + R_{t+1}, \tag{29}$$

the innovation covariance, R_{t+1} the measurement noise covariance at time $t+1$ as defined in Section 2.1, and

$$\overrightarrow{N}_{t+1} = \frac{1}{8}\sum_{i=1}^{8} B\left(\vec{\theta}, \vec{p}; \widehat{\vec{c}}_{i,t+1}\right)\vec{z}_{i,t+1} - \widehat{y}_{t+1}\widehat{x}_{t+1} \tag{30}$$

is the cross-covariance vector.

2. Next, using 23, 28, and 29, we obtain the corrected error covariance:

$$P_{t+1} = \widehat{P}_{t+1} - M_{t+1}\overrightarrow{W}_{t+1}\overrightarrow{W}_{t+1}^T \tag{31}$$

3. Finally, we compute the corrected BOLD signal at time $t+1$ as follows:

$$y_{t+1} = B\left(\vec{\theta}, \vec{p}; \vec{x}_{t+1}\right) \tag{32}$$

REFERENCES

[1] Human brain project. https://www.humanbrainproject.eu/ 2013.

[2] The brain initiative. https://www.whitehouse.gov/BRAIN 2013.

[3] Buxton R, *et al.*. Dynamics of blood flow and oxygenation changes during brain activation: The balloon model. *Magnetic Resonance in Medicine* 1998; **39**:855–864.

[4] Sotero R, Trujillo-Barreto N. Modeling the role of excitatory and inhibitory neuronal activity in the generation of the bold signal. *NeuroImage* 2007; **35**:149–165.

[5] Friston K, *et al.*. Analysis of functional mri time-series. *Human Brain Mapping* 1994; **1**:153–171.

[6] Rajapakse J, *et al.*. Modeling hemodynamic response for analysis of functional mri time-series. *Human Brain Mapping* 1998; **6**:283–300.

[7] Ciuciu P, *et al.*. Unsupervised robust nonparametric estimation of the hemodynamic response function for any fmri experiment. *IEEE Transactions on Medical Imaging* 2003; **22**:1235–1251.

[8] Friston K, *et al.*. Event-related fmri: Characterizing different responses. *NeuroImage* 1998; **7**:30–40.

[9] Lindquist M, Wager T. Modeling the hemodynamic response function using inverse logit functions. *Proceedings of Human Brain Mapping Annual Meeting, 2005*, 2005.

[10] Buxton R, Frank L. A model for the coupling between cerebral blood flow and oxygen metabolism during neural stimulation. *Journal of Cerebral Blood Flow and Metabolism* 1997; **17**:64–72.

[11] Friston K, *et al.*. Nonlinear event-related responses in fmri. *Magnetic Resonance in Medicine* 1998; **39**:41–52.

[12] Friston K, *et al.*. Stochastic design in event-related fmri. *NeuroImage* 1999; **10**:607–619.

[13] Mandeville J, *et al.*. Evidence of a cerebrovascular postarteriole windkessel with delayed compliance. *Journal of Cerebral Blood Flow and Metabolism* 1999; **9**:679–689.

[14] Friston K, *et al.*. Nonlinear responses in fmri: The balloon model, volterra kernels, and other hemodynamics. *NeuroImage* 2000; **12**(4):466–477.

[15] Havlicek M, *et al.*. Dynamic modeling of neural responses in fmri using cubature kalman filtering. *NeuroImage* 2011; **56**(4):2109–2128.

[16] Friston K. Bayesian estimation of dynamical systems: an application to fmri. *NeuroImage* 2002; **16**(2):513–530.

[17] Riera J, *et al.*. A state-space model of the hemodynamic approach: nonlinear filtering of bold signals. *NeuroImage* 2004; **21**(2):547–567.

[18] Johnston L, *et al.*. Nonlinear estimation of the bold signal. *NeuroImage* 2008; **40**(2):504–514.

[19] Murray L, Storkey A. Continuous time particle filtering for fmri. *Advances in Neural Information Processing Systems* 2007; **20**:1–8.

[20] Hu Z, *et al.*. Nonlinear analysis of the bold signal. *EURASIP Journal on Advances in Signal Processing, 2009* 2009; . URL http://asp.eurasipjournals.com/content/2009/1/215409.

[21] Khoram N, *et al.*. Characterization of single-event related brain activity from funtional magnetic resonance imaging (fmri) measurements. *Proc. IEEE Engineering in Medicine and Biology Society, 2014* 2014; :2396–2399.

[22] KJ Friston NTB, Daunizeau J. DEM: A variational treatment of dynamic systems. *NeuroImage* 2008; **41**(3):849–885.

[23] Karam A, *et al.*. Nonlinear neural network for hemodynamic model state and input estimation using fMRI measurements. *Biomedical Signal Processing and Control* 2014; **14**:240–247.

[24] Buxton R, *et al.*. Modeling the hemodynamic response to brain activation. *NeuroImage* 2004; **23**:S220–S233.

[25] Ryan P. Evaluation of a current-based method for disrupting the growth of fibrous tissue around implants: A mathematical and in vivo study. M.s. thesis, California State University, Northridge, Norhtridge, CA 2007.

[26] Galassi M, *et al.*. GNU scientific library reference manual (3rd ed.). http://www.gnu.org/software/gsl/ 2013.

[27] Colton D, Kress R. *Inverse Acoustic and Electromagnetic Scattering Theory*. Springer: Berlin, 1992.

[28] group TFM. SPM 12 manual. http://www.fil.ion.ucl.ac.uk/spm/doc/manual.pdf 2013.

[29] Shmuel A, *et al.*. Negative functional MRI response correlates with decreases in neuronal activity in monkey visual area v1. *Nature Neuroscience* 2008; **9**(4):747–766.